

## Presence of Somatic Mutations in Most Early-Stage Pancreatic Intraepithelial Neoplasia

MITSURO KANDA,\* HANNO MATTHAEI,\* JIAN WU,† SEUNG-MO HONG,\* JUN YU,\* MICHAEL BORGES,\* RALPH H. HRUBAN,\*‡ ANIRBAN MAITRA,\*‡ KENNETH KINZLER,\*‡ BERT VOGELSTEIN,\*‡ and MICHAEL GOGGINS\*.,‡§

\*Department of Pathology, †Department of Oncology, and §Department of Medicine, The Sol Goldman Pancreatic Cancer Research Center, The Johns Hopkins University School of Medicine, Baltimore, Maryland

**More information is needed about genetic factors that initiate development of pancreatic intraepithelial neoplasms—the most common precursors of pancreatic ductal adenocarcinoma. We show that more than 99% of the earliest-stage, lowest-grade, pancreatic intraepithelial neoplasm-1 lesions contain mutations in *KRAS*, *p16/CDKN2A*, *GNAS*, or *BRAF*. These findings could improve our understanding of the development and progression of these premalignant lesions.**

**Keywords:** Pancreatic Cancer; Tumorigenesis; Transformation; Neoplasm.

Pancreatic cancer is the fourth leading cause of cancer death in the United State.<sup>1</sup> Pancreatic intraepithelial neoplasms (PanINs) are the most common precursor to invasive pancreatic adenocarcinoma.<sup>2</sup> They are microscopic lesions (<5 mm diameter), and almost always too small to be identified by current imaging. Low-grade PanINs (PanIN-1) are common and their prevalence increases with age, whereas high-grade PanINs are uncommon and usually are found in pancreata with invasive pancreatic cancer. Multiple PanINs of all grades frequently are observed in individuals with inherited susceptibility to pancreatic cancer.<sup>3</sup> More than 90% of invasive adenocarcinomas of the pancreas harbor oncogenic mutations in *KRAS* whereas *BRAF* mutations occur in a small subset of *KRAS*-wild-type pancreatic cancers.<sup>1,4</sup> Almost all invasive pancreatic cancers inactivate *p16/CDKN2A*. *GNAS* is mutated in approximately 60% of intraductal papillary mucinous neoplasms (IPMNs), and in some invasive pancreatic cancers arising in association with an IPMN.<sup>5</sup> Several genetic alterations identified in invasive pancreatic adenocarcinomas also are present in PanINs, with evidence of increasing prevalence of these alterations with PanIN grade.<sup>2</sup> However, the genes responsible for early PanIN development remain poorly understood. Thus, a meta-analysis evaluating studies of mutant *KRAS* prevalence in PanINs found that among patients with pancreatic ductal adenocarcinoma, *KRAS* mutations were detected by conventional methods in 36% of PanIN-1A, 44% of PanIN-1B, and 87% of high-grade PanIN lesions (PanIN-2 and PanIN-3).<sup>6</sup> Data such as these indicate that *KRAS* mutations are more involved after PanIN initiation; genetic alterations that initiate tumorigenesis should have the same prevalence, independent of grade.

The goal of the current study was to use more sensitive mutation detection methods to obtain a more detailed genetic understanding of early PanIN development. For this purpose, first we used laser capture to microdissect 169 PanINs (50 PanIN-1A, 52 PanIN-1B, 45 PanIN-2, and 22 PanIN-3 lesions) from 89 patients with benign and malignant pancreatic diseases (Supplementary Table 1; Figure 1A), invasive pancreatic ductal adenocarcinomas from 12 patients, and normal pancreatic ducts from 20 patients. After DNA isolation and whole-genome amplification, DNA was analyzed for somatic mutations in *KRAS*, *BRAF*, *GNAS*, and *p16/CDKN2A* using pyrosequencing and high-resolution melt-curve analysis. The limit of detection of these assays is approximately 5% (ie, mutant alleles can be detected at concentrations of 5% or more [mutant: wild-type alleles, 1:20, cells, 1:10]) (see Supplementary Materials and Methods section).

By using pyrosequencing, *KRAS* codon 12 mutations were detected in 46 (92.0%) of 50 PanIN-1A, 48 (92.3%) of 52 PanIN-1B, 42 (93.3%) of 45 PanIN-2, and 21 (95.4%) of 22 PanIN-3 lesions (Supplementary Table 2). Occasional mutations of *KRAS* codon 13 and codon 61 were identified (Supplementary Table 2), and a second nondominant *KRAS* mutation was found in 6 of 169 PanINs. No evidence of *KRAS* amplification was found. Melt-curve analysis confirmed the presence of *KRAS* gene mutations in every sample that was positive by pyrosequencing (Supplementary Figure 1A). Overall, 163 of 169 (96.4%) PanINs harbored *KRAS* mutations. No *KRAS* mutations were identified in normal pancreatic duct samples (Supplementary Table 2). Five of the 169 PanIN lesions tested by pyrosequencing had a second minor *KRAS* codon 12 mutation. Many PanIN-1 lesions had low mutant *KRAS* concentrations (mean, ~20% of alleles by pyrosequencing, Supplementary Table 3), perhaps explaining why prior studies reported a lower prevalence of *KRAS* mutations in low-grade PanINs. To check the purity of our laser capture microdissection, we repeated the microdissections from 16 of the PanINs, using another set of slides. The mutant *KRAS* concentrations in DNA from the second

**Abbreviations used in this paper:** IPMN, intraductal papillary mucinous neoplasm; PanIN, pancreatic intraepithelial neoplasm; PanIN-1, low-grade pancreatic intraepithelial neoplasm.

© 2012 by the AGA Institute

0016-5085/\$36.00

doi:10.1053/j.gastro.2011.12.042

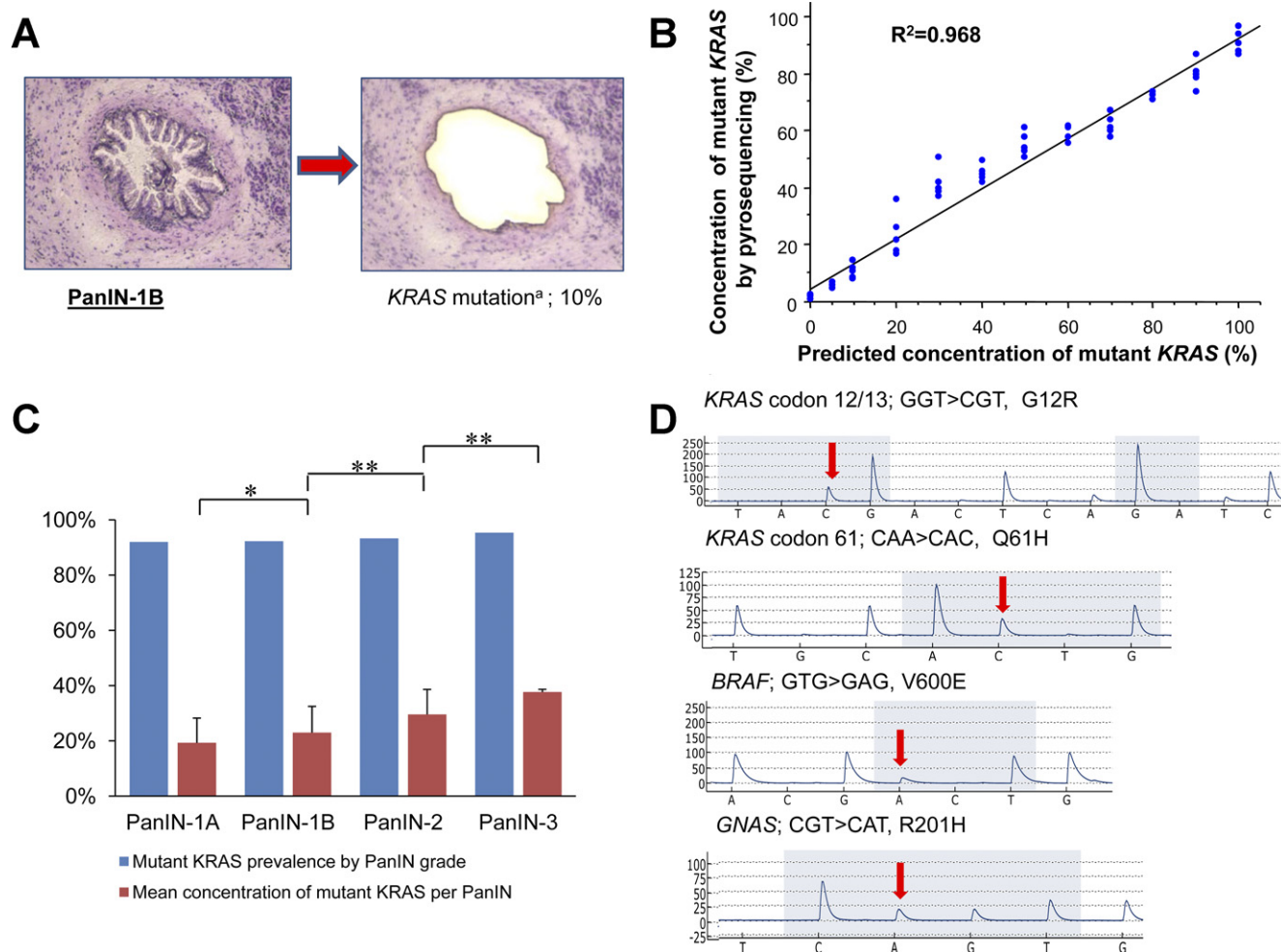


**Figure 1.** (A) An example of an H&E-stained PanIN before and after laser capture microdissection. Microdissection was performed at the duct epithelial cell borders to avoid contamination with stromal cells. <sup>a</sup>Concentrations of mutant DNA were by pyrosequencing. (B) Scatterplot graph of actual and predicted concentrations of mutant DNA by pyrosequencing. (C) Prevalence of *KRAS* codon 12 mutations and concentration of mutations per PanIN by grade of PanIN. *KRAS* codon 12 mutations were found in more than 92% of PanINs in every group. The average percentage of mutant *KRAS* alleles within a PanIN increased at each PanIN grade. (D) Representative pyrosequencing traces with mutant sequences highlighted by arrows. \* $P < .05$ , \*\* $P < .001$ .

microdissection were not significantly different from those of the first microdissections (Supplementary Materials and Methods). We also analyzed mutant *KRAS* concentrations in invasive pancreatic adenocarcinomas, and these samples had close to the concentrations of mutant *KRAS* one would expect if they consisted entirely of *KRAS*-mutant cancer cells without any contaminating wild-type (and presumably non-neoplastic) cells (mean, 42.5% of *KRAS* alleles, not significantly different from the mean mutant *KRAS* allele concentration in PanIN-3 lesions). Indeed, we found that the average concentration of mutant *KRAS* alleles in PanINs increased significantly with increasing grade of PanIN (Figure 1C, Figure 2).

These results indicate that virtually all PanINs harbor *KRAS* mutations. However, in the earliest PanIN lesions, these mutations are generally present in only a fraction of the cells comprising the lesion. The percentage of mutant *KRAS* cells in the PanIN progressively increases with the PanIN grade, consistent with a gradual expansion of the *KRAS*-mutant clone as the PanIN progresses.

We then sought to determine if mutations in other genes are present in the few *KRAS*-wild-type PanINs, particularly low-grade PanINs. Because prior studies have found that *TP53* and *SMAD4* mutations do not appear until late in the neoplastic progression, we focused on *BRAF* because it sometimes is mutant in *KRAS* wild-type cancers; on *p16/CDKN2A* because loss of *p16/CDKN2A* expression has been found in some early PanINs; and *GNAS* because it commonly is mutated in another type of premalignant pancreatic lesion (IPMNs).<sup>5</sup>

Although *p16/CDKN2A* mutations were identified in only 17 of 147 PanIN-1/2 lesions (11.5%), they were detected more often in *KRAS*-wild-type PanINs than in *KRAS*-mutant PanINs ( $P = .0209$ ). A similar trend was noted for *GNAS* mutations, which were the only mutations identified in 2 PanINs ( $P = .0886$ ; Figure 2). Interestingly, similar to what was found for some IPMNs,<sup>5</sup> among PanIN-1/2 lesions with both *GNAS* and *KRAS* mutations, mutant *GNAS* concentrations were higher than mutant *KRAS* ( $P = .0084$ , paired  $t$  test) (Supplemen-

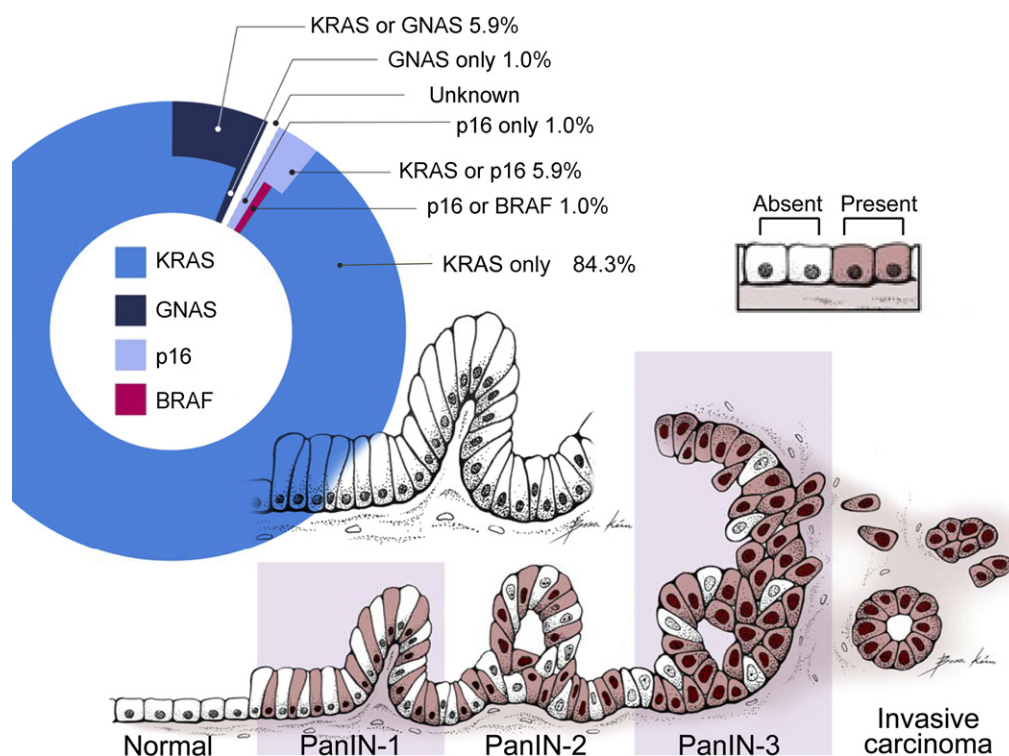


**Figure 2.** Initial mutations of PanIN-1 lesions. The pie chart in the upper portion of the figure indicates the percentage of mutations in each of the genes tested (*KRAS*, *GNAS*, *p16*, and *BRAF*) identified in PanIN-1 lesions. For PanIN-1 lesions with more than one mutation, we could not determine which gene was mutated first. For example, a few PanIN-1 lesions had both a *KRAS* mutation and a *GNAS* mutation, so the initial mutation in these PanINs was indicated as arising in either *KRAS* or *GNAS*. The bottom portion of the figure is a schematic model illustrating the increasing percentage of mutant *KRAS* cells within PanIN lesions as they progress from a low-grade to a high-grade PanIN and to an invasive ductal adenocarcinoma, based on measurements of the average mutant *KRAS* concentrations per PanIN. Shaded cells (present) represent PanIN cells with mutant *KRAS*, and nonshaded cells (absent) represent PanIN cells without mutant *KRAS* (wild-type).

tary Table 2), suggesting that low mutant *KRAS* concentrations in PanIN samples were not simply the result of contamination with DNA from nearby stromal cells. It also suggests that in some PanINs, the *KRAS* mutation arose later than the *GNAS* mutation. There were no histologic differences in cell morphology within PanIN-1 lesions with low vs high concentrations of either mutant *KRAS* or *GNAS* (Supplementary Figure 1). *GNAS* mutations were detected more often in PanINs from patients with a diagnosis other than pancreatic adenocarcinoma ( $P = .0398$ ). Overall, we were able to identify at least one mutation in *KRAS*, *GNAS*, *p16/CDKN2A*, or *BRAF* in all but 1 of 169 PanINs (Supplementary Tables 1 and 2). No mutant *KRAS* or *GNAS* was detected in this one wild-type PanIN (patient 72), even with the sensitive techniques we used (detection limit <1%).

To confirm the prevalence of *KRAS* and *GNAS* mutations in PanINs, we also conducted an independent analysis of an additional 37 PanIN lesions (11 PanIN-1, 20 PanIN-2, and 7 PanIN-3 lesions) using 2 additional ultrasensitive technologies: digital ligation (limit of detection, 1/200 alleles) and Beads, Emulsion, Amplification (BEAM)ing (limit of detection, 1/1000 alleles) (Supplementary Materials and Methods), and found *KRAS* mutations in 94.6% of PanINs and *GNAS* mutations in 11.4% (Supplementary Table 4), with complete concordance of

the mutation results with both platforms. A second non-dominant *KRAS* mutation was found more often using these methods than by pyrosequencing, consistent with the lower limit of detection of these assays.

These results indicate that somatic mutations are required for the early development of virtually all PanINs. Our results are consistent with observations in genetically engineered mouse models in which mouse PanINs can be initiated by oncogenic *KRAS*.<sup>7</sup> Although low-grade PanIN cells have some metaplastic features, our results do not support the hypothesis that PanINs begin as metaplasias and only subsequently acquire genetic alterations. If this were true, more low-grade (early) PanINs would lack oncogenic mutations. (We found only 1 of 102 PanIN-1 lesions lacked a mutation.) In prior studies, we have examined the metaplastic lesion known as acinar-to-ductal metaplasia for evidence of genetic alterations (mutant *KRAS* and telomere length analysis) and did not find evidence from this analysis that acinar-to-ductal metaplasias are precursors to PanINs. The findings that many low-grade PanINs contain mixtures of mutant and wild-type *KRAS* cells, that *GNAS* mutation concentrations can be higher than *KRAS* mutation concentrations in the same PanIN, and that the average proportion of mutant *KRAS* within PanINs increases with PanIN grade, suggests that mutant *KRAS* alone provides only a modest selective

advantage over neighboring cells. This finding suggests that the *KRAS*-mutant clone is partially restrained within the PanIN, possibly by oncogene-induced senescence<sup>8,9</sup> and this restraint likely is maintained until additional genetic and/or epigenetic events (such as *p16/CDKN2A* inactivation) occur. The driving force behind the expansion of cells within PanINs that do not harbor mutant *KRAS* is not certain. One possibility is that PanIN-initiating event(s) precede oncogenic *KRAS* mutations. However, our genome<sup>4</sup> and methylome<sup>10</sup> studies indicate there are no other commonly mutated or epigenetically silenced<sup>10</sup> genes in pancreatic cancers that stand out as candidate initiators of PanIN development. Telomere shortening is observed in almost all low-grade PanINs<sup>11</sup> but this phenomenon could be a consequence of activation of oncogene stress-induced senescence programs<sup>12</sup> rather than an initiator of PanINs.

One unifying hypothesis to explain all these observations is that *KRAS*, and occasionally *p16/CDKN2A*, *GNAS*, or *BRAF*, mutations can initiate PanIN development, and that these mutant cells induce surrounding cells to proliferate. Such proliferation could come from autocrine and paracrine influences from *KRAS*-mutant PanIN cells, such as expression of sonic hedgehog, and other developmental genes,<sup>13,14</sup> as well as stress-inducing signals that lead to senescence,<sup>15</sup> and induce metaplastic features in PanIN epithelial cells including adjacent cells lacking *KRAS* mutations.

### Supplementary Material

Note: To access the supplementary material accompanying this article, visit the online version of *Gastroenterology* at [www.gastrojournal.org](http://www.gastrojournal.org), and at doi: 10.1053/j.gastro.2011.12.042.

### References

1. Vincent A, et al. *Lancet* 2011;378:607–620.
2. Hruban RH, et al. *Clin Cancer Res* 2000;6:2969–2972.
3. Shi C, et al. *Clin Cancer Res* 2009;15:7737–7743.
4. Jones S, et al. *Science* 2008;321:1801–1806.
5. Wu J, et al. *Sci Transl Med* 2011;3:92ra66.
6. Lohr M, et al. *Neoplasia* 2005;7:17–23.
7. Hingorani SR, et al. *Cancer Cell* 2003;4:437–450.
8. Caldwell ME, et al. *Oncogene* 2011 Aug 22 [Epub ahead of print].
9. Lee KE, et al. *Cancer Cell* 2010;18:448–458.
10. Vincent A, et al. *Clin Cancer Res* 2011;17:4341–4354.
11. van Heek NT, et al. *Am J Pathol* 2002;161:1541–1547.
12. Ben-Porath I, et al. *J Clin Invest* 2004;113:8–13.
13. Strobel O, et al. *Gastroenterology* 2010;138:1166–1177.
14. Prasad NB, et al. *Cancer Res* 2005;65:1619–1626.
15. Kuilman T, et al. *Nat Rev Cancer* 2009;9:81–94.

---

Received October 20, 2011. Accepted December 22, 2011.

#### Reprint requests

Address requests for reprints to: Michael Goggins, MD, Department of Pathology, Johns Hopkins Medical Institutions, 1550 Orleans Street, Baltimore, Maryland 21231. e-mail: [mgoggins@jhmi.edu](mailto:mgoggins@jhmi.edu); fax: (410) 614-0671.

#### Acknowledgments

The authors thank Ms Bona Kim for providing the pancreatic intraepithelial neoplasm illustration (Figure 2).

M.K., H.M., and J.W. contributed equally to this work.

#### Conflicts of interest

The authors disclose no conflicts.

#### Funding

This work was supported by National Institutes of Health grants (CA62924, R01CA97075, R01CA120432, RC2CA148376, and P01CA134292), the Stringer Foundation, the Michael Rolfe Foundation, the Lustgarten Foundation for pancreatic cancer research, and German Cancer Aid (Deutsche Krebshilfe e.V.).

## Supplementary Materials and Methods

All elements of this investigation were approved by The Johns Hopkins Medical Institutional Review Board and written informed consent was obtained from all patients.

### Laser Capture Microdissection

PanINs were identified at the time of frozen-section analysis of pancreatic resection specimens by R.H.H. from 2007 to 2010 as microscopic papillary or flat non-invasive epithelial neoplasms arising in a pancreatic duct, composed of cuboidal to columnar cells with varying amounts of mucin and degrees of cytologic and architecture atypia. PanINs were graded further into PanIN-1A, PanIN-1B, PanIN-2, and PanIN-3 lesions based on the degree of cytologic and architectural atypia.<sup>1</sup> Frozen sections were placed on ultraviolet-irradiated, membrane-coated slides (Carl Zeiss Microimaging, München, Germany). Slides were stained with H&E. Briefly, nuclei were stained with hematoxylin (Sigma-Aldrich, St. Louis, MO) for 10 minutes, and the cytoplasm was stained with eosin (Sigma-Aldrich) for 5 minutes after consecutive rehydration with 100%, 96%, and 70% ethanol for 1 minute each. The stained slides were microdissected within 2 hours by an LCM system (Leica LMD7000; Leica, Buffalo Grove, IL). Care was taken to ensure that PanINs were not pooled inadvertently. Pancreatic ducts that contained 2 different grades of PanINs within the same duct were excluded from dissection. We did not pool dissections of PanIN cells from different ducts even when they were on the same slide; these are probably different from PanINs. Because each tissue section is only 10- $\mu$ m/L thick, a PanIN lesion is typically many sections deep. Therefore, we typically dissected cells from one PanIN from several adjacent slides (3–5 slides). Usually, a PanIN can be followed along adjacent tissue sections and can be identified from landmarks such as the shape of the duct and the morphology of the cells and of the surrounding areas of acinar cells and islets. In the first set of cases, 50 PanIN-1A, 52 PanIN-1B, 45 PanIN-2, and 22 PanIN-3 were obtained from 89 individual patients, including 53 patients with pancreatic ductal adenocarcinoma (Supplementary Table 1). In the second set of cases, 37 PanINs were analyzed (11 PanIN-1, 20 PanIN-2, and 7 PanIN-3 lesions) from 32 individuals (Supplementary Table 3).

### DNA Extraction and Whole-Genome Amplification

Genomic DNA was extracted from the microdissected tissues using the QIAamp DNA Micro Kit (Qiagen, Valencia, CA). Whole-genome amplification was conducted for all extracted DNA samples with REPLI-g Mini Kit (Qiagen) and incubation time was 16 hours. DNA samples were quantified by Quantifiler (Applied Biosystems, Foster City, CA) before and after whole-genome amplification.

### Pyrosequencing

The mutational status of *KRAS*, *GNAS*, and *BRAF* was investigated by pyrosequencing. Ten nanograms of whole-genome amplified DNAs were polymerase chain reaction amplified with the PyroMark polymerase chain reaction Kit (Qiagen) according to the manufacturer's protocol. After amplification, 20  $\mu$ L of biotinylated polymerase chain reaction product was immobilized on streptavidin-coated sepharose beads (streptavidin sepharose high performance; GE Health care Bio-Sciences Corp, Piscataway, NJ). The purified biotinylated polymerase chain reaction product was released into the PyroMark Q24 (Biotage AB, Uppsala, Sweden) with PyroMark Gold reagents (Qiagen) containing 0.3  $\mu$ mol/L sequencing primer and annealing buffer. In addition to detection of mutations of each gene, the peaks of pyrograms, indicating populations of mutant, were investigated in all samples. To determine the limit of detection of pyrosequencing for *KRAS* mutations, a stepwise dilution series (0%, 5%, 10%, 20%, 30%, 40%, 50%, 60%, 70%, 80%, 90%, and 100%) was performed using the MiaPaCa2 pancreatic cancer cell line known to have a homozygous *KRAS* mutation (GGT>GTT, G12V). This analysis showed that pyrosequencing could identify mutant *KRAS* concentrations of 5% or more and accurately reflect mutant concentrations (Figure 1B). To ensure that we accurately determined samples with low mutant *KRAS* concentrations, any samples with less than 10% mutant *KRAS* concentrations were rechecked by repeating the laser capture microdissection of adjacent slides of the same PanIN and then repeating the pyrosequencing. Representative pyrograms are shown in Figure 1D. There was no significant difference in mutant *KRAS* concentrations in the paired samples (Student paired *t* test). Although each PanIN was dissected to avoid all contaminating normal stromal cells, to ensure that our microdissections were not removing stromal cells near the basement membrane of the PanINs, we next repeated the laser microdissections of 6 PanIN lesions, this time dissecting the cytoplasm of the PanINs to avoid the basement membrane and any adjacent stromal cells. Again, we found no significant difference in mutant *KRAS* concentrations between these microdissected samples and the previous microdissections of the same PanINs.

### High-Resolution Melt-Curve Analysis

The mutational status of exons 1–2 of *p16/CDKN2A* was investigated with high-resolution melt-curve analysis. High-resolution melt-curve analysis targeting *KRAS* codons 12 and 13 also was performed on all samples to confirm results of the *KRAS* pyrosequencing. The polymerase chain reactions for high-resolution melt-curve analysis were 5  $\mu$ L volume for each well containing 10 ng of whole-genome amplified DNAs, 2 $\times$  concentration amplification buffer (Invitrogen, Carlsbad, CA), 0.3 mmol/L deoxynucleoside triphosphate mix, 1 mmol/L

MgSO<sub>4</sub>, 0.02 U/ $\mu$ L Platinum pfx polymerase (Invitrogen), 8% dimethyl sulfoxide, 0.1 U/ $\mu$ L LcGreen<sup>+</sup> dye (Idaho Tech, Salt Lake City, UT), and 200 nmol/L forward and reverse primers. All samples were tested in triplicate. In each polymerase chain reaction plate, 5 wells were allocated to wild-type control DNA and 1 well to nontemplate control to validate the polymerase chain reaction. For the *KRAS* assay, 3 wells of MiaPaCa2 DNA was included as a positive control for mutant *KRAS*. The germline DNA of patients with positive PanIN high-resolution melt-curve analysis results for *p16/CDKN2A* mutations also was analyzed by high-resolution melt-curve analysis or sequenced using Sanger sequencing to identify any germline *p16/CDKN2A* variants. No germline *p16/CDKN2A* variants were identified. After the polymerase chain reaction, the plate was transferred immediately to the LightScanner mutation analyzer (Idaho Tech), setting a melt temperature range between 72°C and 98°C. Scanning data were analyzed by the LightScanner software. A fluorescence difference of 5% was set as a cut-off level for identifying variant samples as suggested in previous reports and confirmed by our own dilution curves with positive controls.<sup>2</sup> Representative results of high-resolution melt-curve analysis are shown in Supplementary Figure 1B. For the 6 PanINs in the first set of 169 PanINs found to be wild-type for *KRAS*, we used digital melt curve analysis to test for low mutant DNA concentrations using the same conditions described earlier but analyzing PanIN DNA in 96 wells and 10 genome equivalents per well (limit of detection, <1%).<sup>3</sup> No mutations in *KRAS* were identified in any of these PanINs. For the one PanIN in the first set of 169 PanINs that was wild-type for all 4 genes tested, we also used digital melt curve analysis to test for low mutant DNA concentrations of *GNAS*. No *GNAS* mutation was identified in this PanIN.

### ***KRAS* Amplification**

Aberrant *KRAS* amplification was evaluated with real-time quantitative polymerase chain reaction. Ten nanograms of DNA samples of wild-type control, positive control (Pa08C, pancreatic cancer cell line with aberrantly increased *KRAS* amplification), and PanIN samples were used as a template after being quantified precisely by the Quantifiler. Real-time detection of the emission

intensity of SYBR Green was performed with the 7900HT Fast Real-Time polymerase chain reaction System (Applied Biosystems). Threshold cycles (Ct value) of samples were compared between wild-type control, positive control, and PanIN samples.

### ***Digital Ligation Assay for KRAS and GNAS Mutations***

Digital ligation was used to identify *KRAS* codon 12 and *GNAS* codon 201 mutations on the independent set of 37 PanINs and was performed as previously described.<sup>4</sup>

### ***BEAMing***

BEAMing assays were performed on the independent set of 37 PanINs to confirm the digital ligation results as previously described.<sup>5</sup>

### ***Primers***

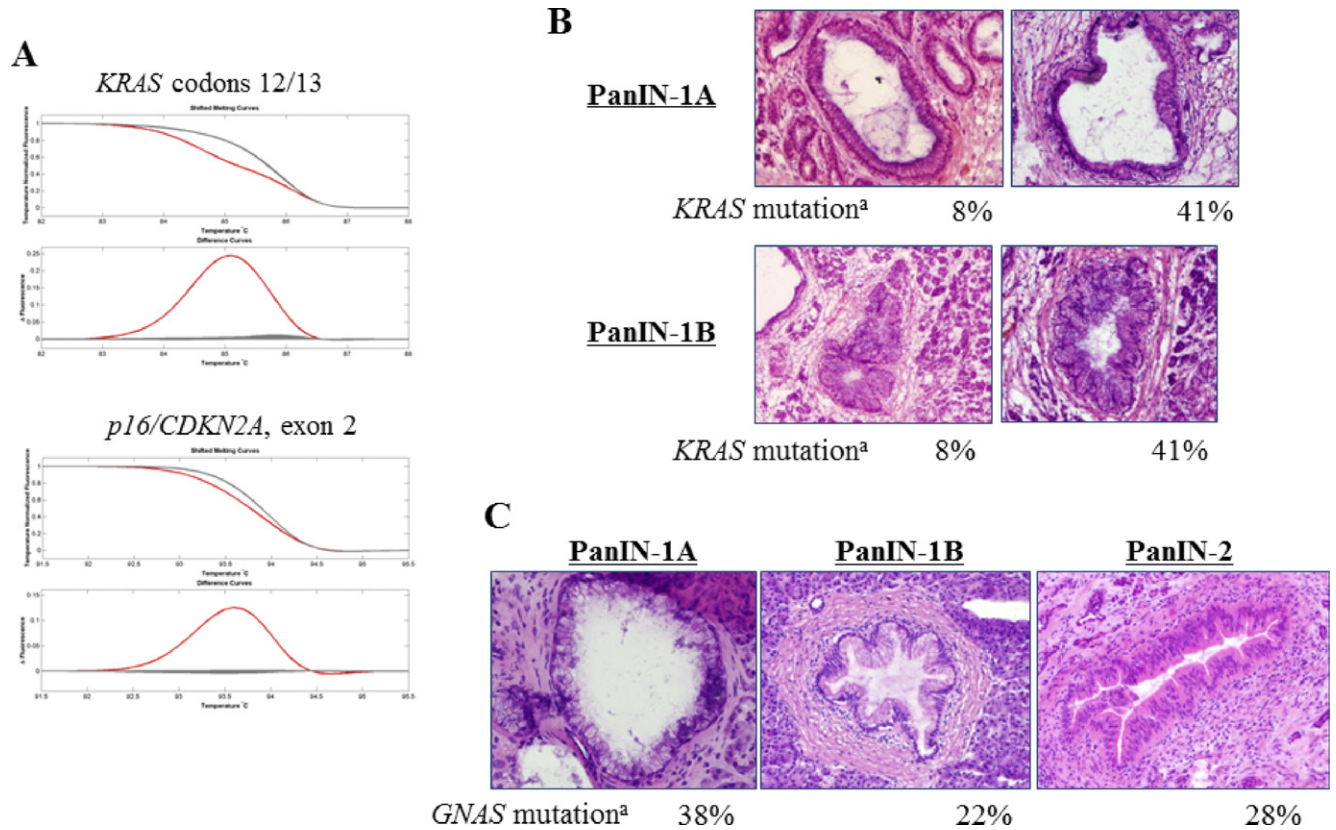
The sequences of the PCR primers used in this study are and their conditions are provided in Supplementary Table 5.

### ***Statistical Analysis***

Mean pyrogram peaks of each PanIN group were compared with the Mann–Whitney *U* test. We used a paired *t* test to analyze the differences in concentration of mutant between *KRAS* codon 12 and *GNAS*. The correlation between mutational status of the PanIN and the pathologic diagnosis of the lesion that led to the patient's pancreatic resection was analyzed by the Fisher exact test. Association of mutational status of each gene also was analyzed by the Fisher exact test. Statistical analysis was performed using SPSS Statistics 17.0 software (SPSS, Chicago, IL). A *P* value of less than .05 was considered statistically significant.

### **Supplementary References**

1. Hruban RH, et al. *Am J Surg Pathol* 2001;25:579–586.
  2. Erali M, et al. *Methods* 2010;50:250–261.
  3. Zou H, et al. *Gastroenterology* 2009;136:459–470.
  4. Wu J, et al. *Sci Transl Med* 2011;3:92ra66.
  5. Diehl F, et al. *Nat Med* 2008;14:985–990.
-



**Supplementary Figure 1.** (A) Shifted melt curves and difference curves of high-resolution melt curve analysis of *KRAS* codons 12/13 and exon 2 of *p16/CDKN2A*. PanINs with mutation were detected as red curves. (B) Representative microscopic findings of PanINs with *KRAS* codon 12 mutation. There was no evident histologic difference between PanINs with low and high concentrations of mutant *KRAS*. (C) Representative microscopic images of PanINs with *GNAS*. No morphologic differences were found between *GNAS* mutant and *KRAS* mutant PanINs. <sup>a</sup>Concentrations of mutant *KRAS* or *GNAS* by pyrosequencing.

**Supplementary Table 1.** List of Patients Enrolled in This Study

	Sex	Age	Pathologic diagnosis	PanINs analyzed
1	Male	70	Ductal adenocarcinoma	PanIN-1A, 2
2	Male	60	IPMN	PanIN-1A
3	Male	69	Ductal adenocarcinoma	PanIN-1B
4	Male	65	Cholangiocarcinoma	PanIN-1A, 2, 3
5	Male	72	Duodenum adenocarcinoma	PanIN-1A, 2
6	Female	74	Chronic pancreatitis	PanIN-1A, 1B, 2
7	Female	66	Ductal adenocarcinoma	PanIN-1A, 2
8	Male	76	Bile duct adenoma	PanIN-1B
9	Female	79	Ductal adenocarcinoma	PanIN-1A
10	Female	76	Ductal adenocarcinoma	PanIN-1B, 2
11	Male	69	Ductal adenocarcinoma	PanIN-1B, 2
12	Female	72	Ductal adenocarcinoma	PanIN-1A
13	Male	50	Ductal adenocarcinoma	PanIN-3
14	Female	67	Pancreatic endocrine neoplasm	PanIN-1B, 2
15	Male	62	IPMN	PanIN-1B <sup>a</sup>
16	Female	37	Chronic pancreatitis	PanIN-1A
17	Female	56	Ductal adenocarcinoma	PanIN-1A
18	Male	85	Metastatic neoplasm	PanIN-1A, 2
19	Male	63	Ductal adenocarcinoma	PanIN-1A, 2
20	Female	69	Ductal adenocarcinoma	PanIN-1B, 2 <sup>a</sup>
21	Male	83	Metastatic neoplasm	PanIN-1A, 1B, 2
22	Male	61	Serous cystadenoma	PanIN-2
23	Female	71	Ductal adenocarcinoma	PanIN-1B
24	Female	74	Ductal adenocarcinoma	PanIN-1A, 1B, 2
25	Female	76	Ductal adenocarcinoma	PanIN-1B
26	Female	60	Chronic pancreatitis	PanIN-1A
27	Male	79	Ductal adenocarcinoma, IPMN	PanIN-1A
28	Female	58	Pancreatic endocrine neoplasm	PanIN-1A
29	Male	62	Adenosquamous carcinoma	PanIN-1B, 2
30	Female	51	IPMN	PanIN-1B
31	Female	58	IPMN	PanIN-1A, 2
32	Male	61	IPMN	PanIN-1B
33	Female	65	Ductal adenocarcinoma	PanIN-3
34	Male	50	Ductal adenocarcinoma	PanIN-1B, 2
35	Female	64	Ductal adenocarcinoma	PanIN-1A, 1B, 2
36	Female	52	IPMN	PanIN-1A, 3
37	Female	66	Ductal adenocarcinoma	PanIN-1A
38	Female	66	Chronic pancreatitis	PanIN-1B, 2, 3
39	Female	58	IPMN	PanIN-1B <sup>a</sup>
40	Male	63	Ductal adenocarcinoma	PanIN-2
41	Male	55	IPMN	PanIN-1B
42	Female	67	Pancreatic endocrine neoplasm	PanIN-1B
43	Female	60	Ductal adenocarcinoma	PanIN-1A, 1B, 2
44	Female	69	Ductal adenocarcinoma	PanIN-1A, 1B, 2, 3
45	Female	66	Ductal adenocarcinoma	PanIN-1B, 2
46	Female	59	Ductal adenocarcinoma	PanIN-2, 3
47	Male	76	IPMN	PanIN-2, 3
48	Male	75	Ductal adenocarcinoma	PanIN-1B, 2, 3
49	Female	45	Ductal adenocarcinoma	PanIN-1A, 1B, 2
50	Male	65	IPMN	PanIN-1A, 1B, 2
51	Female	55	Ductal adenocarcinoma	PanIN-1A, 1B
52	Male	85	IPMN	PanIN-1A, 1B
53	Male	74	Ductal adenocarcinoma	PanIN-2, 3
54	Female	52	Serous cystadenoma	PanIN-1A, 1B
55	Female	62	Pancreatic endocrine neoplasm	PanIN-1B
56	Female	75	Chronic pancreatitis	PanIN-1B, 2
57	Female	56	IPMN	PanIN-1A, 1B, 2
58	Female	70	Ductal adenocarcinoma	PanIN-1A, 1B

**Supplementary Table 1.** Continued

	Sex	Age	Pathologic diagnosis	PanINs analyzed
59	Female	78	Ductal adenocarcinoma	PanIN-2, 3
60	Female	63	Ductal adenocarcinoma	PanIN-3
61	Female	54	Ductal adenocarcinoma	PanIN-3
62	Female	64	Ductal adenocarcinoma	PanIN-2, 3
63	Male	73	Ductal adenocarcinoma	PanIN-1A, 1B
64	Female	73	Ductal adenocarcinoma	PanIN-1A, 1B, 2
65	Male	55	Pancreatic endocrine neoplasm	PanIN-1A, 1B
66	Male	59	Ductal adenocarcinoma	PanIN-1A, 1B
67	Female	61	Chronic pancreatitis	PanIN-1A, 1B
68	Male	68	Ductal adenocarcinoma	PanIN-1A, 1B, 2
69	Female	89	Ductal adenocarcinoma	PanIN-1A, 1B
70	Female	86	Serous cystadenoma	PanIN-1A, 1B
71	Male	73	Ductal adenocarcinoma	PanIN-1A, 2, 3
72	Female	58	Mucinous cystadenoma	PanIN-1A <sup>a,b</sup>
73	Female	60	Ductal adenocarcinoma	PanIN-1A, 1B
74	Male	57	Ductal adenocarcinoma	PanIN-2 <sup>a</sup>
75	Female	63	Ductal adenocarcinoma	PanIN-1A, 1B, 2
76	Female	63	Ampullary adenoma	PanIN-1A, 1B
77	Female	71	Ductal adenocarcinoma	PanIN-1A, 1B
78	Female	60	Ductal adenocarcinoma, IPMN	PanIN-3
79	Female	63	Ductal adenocarcinoma	PanIN-3
80	Female	54	Ductal adenocarcinoma	PanIN-1A, 1B, 2
81	Male	58	Ductal adenocarcinoma	PanIN-2, 3
82	Male	63	Chronic pancreatitis	PanIN-1B
83	Male	63	Ductal adenocarcinoma	PanIN-1A, 1B, 2
84	Male	73	Ductal adenocarcinoma	PanIN-1A, 1B, 2, 3
85	Male	72	Ductal adenocarcinoma	PanIN-1A, 1B, 3
86	Female	69	Ductal adenocarcinoma	PanIN-1A, 1B, 2, 3
87	Male	49	Ductal adenocarcinoma	PanIN-3
88	Male	75	Ductal adenocarcinoma	PanIN-2
89	Female	58	IPMN	PanIN-1A, 2

<sup>a</sup>Highlighted PanINs were *KRAS* wild-type.

<sup>b</sup>No mutations identified in any gene tested.

**Supplementary Table 2.** Frequency of Mutation in Each Gene

	<i>KRAS</i> codon 12 WT; GGT	<i>KRAS</i> codon 13 WT; GGC	<i>KRAS</i> codon 61 WT; CAA	<i>KRAS</i> codon 146 WT; GCA	<i>BRAF</i> codon 600 WT; GTG	<i>GNAS</i> codon 201 WT; CGT	<i>p16/CKDN2A</i>
Normal duct	0%	0%	0%	0%	0%	0%	0%
PanIN-1A	92.0% (46/50) CGT 8 GAT 16 GTT 21 TGT 1	2.0% (1/50) GAC 1	4.0% (2/50) CGA 1 CTA 1	0%	0%	8.0% (4/50) CAT 2 TGT 2	6.0% (3/50) Exon1 1 Exon2 2
PanIN-1B	92.3% (48/52) CGT 9 GAT 21 GTT 17 TGT 1	0%	1.9% (1/52) CAC 1	0%	1.9% (1/52) GAG 1	5.8% (3/52) CAT 1 TGT 2	9.6% (5/52) Exon1 3 Exon2 2 Exon1, 2 1
PanIN-2	93.3% (42/45) CGT 6 GAT 20 GTT 14 TGT 2	0%	2.2% (1/45) CGA 1	0%	0%	13.3% (6/45) CAT 4 TGT 2	20.0% (9/45) Exon1 3 Exon2 5 Exon1, 2 1
PanIN-3	95.4% (21/22) CGT 2 GAT 12 GTT 7	4.5% (1/22) AGC 1	9.1% (2/22) CAT 1 CGA 1	0%	4.5% (1/22) GAG 1	4.5% (1/22) CAT 1	36.4% (7/22) Exon1 3 Exon2 3 Exon1, 2 1

WT, wild-type.

**Supplementary Table 3.** Concentrations of Mutant *KRAS*

<i>KRAS</i> mutation	PanIN-1A (n = 50)	PanIN-1B (n = 52)	PanIN-2 (n = 45)	PanIN-3 (n = 22)	Pancreatic cancer (n = 12)
Codon 12	7%	10%	21%	28%	37%
GGT>CG	10%	18%	22%	38%	81%
T	16%	20%	31%		
(G12R)	24%	23%	31%		
	24%	30%	34%		
	25%	30%			
	30%	31%			
	35%	32%			
		46%			
Mean ± SD	21.4% ± 9.7%	26.7% ± 10.3%	29.3% ± 6.5%	33.0% ± 7.1%	59.0% ± 33.1%
Codon 12	8%	6%	20%	24%	25%
GGT>G	8%	8%	21%	27%	31%
AT	9%	8%	22%	33%	46%
(G12D)	10%	12%	24%	34%	55%
	12%	15%	24%	36%	
	14%	15%	25%	39%	
	16%	15%	26%	40%	
	18%	15%	26%	41%	
	18%	16%	28%	44%	
	22%	16%	28%	46%	
	25%	16%	29%	50%	
	27%	19%	31%	54%	
	29%	19%	31%		
	31%	20%	32%		
	41%	25%	33%		
	42%	30%	36%		
		30%	39%		
		30%	40%		
		32%	42%		
		33%	44%		
		36%			
Mean ± SD	20.6% ± 11.1%	19.8% ± 8.9%	30.1% ± 7.1%	39.0% ± 8.9%	39.3% ± 13.7%
Codon 12 GGT>GTT (G12V)	6%	15%	21%	29%	26%
	7%	16%	22%	31%	29%
	7%	16%	23%	33%	37%
	11%	17%	24%	38%	41%
	11%	18%	26%	39%	
	11%	18%	27%	42%	
	13%	18%	30%	46%	
	13%	19%	32%		
	17%	22%	33%		
	18%	24%	35%		
	18%	24%	35%		
	20%	26%	38%		
	20%	33%	42%		
	20%	36%			
	21%	38%			
	23%	41%			
	23%	45%			
	24%				
	25%				
	25%				
	30%				

**Supplementary Table 3.** Continued

<i>KRAS</i> mutation	PanIN-1A (n = 50)	PanIN-1B (n = 52)	PanIN-2 (n = 45)	PanIN-3 (n = 22)	Pancreatic cancer (n = 12)
Mean $\pm$ SD	17.3% $\pm$ 6.8%	25.1% $\pm$ 9.8%	30.9% $\pm$ 7.4%	36.9% $\pm$ 6.1%	33.3% $\pm$ 6.9%
Codon 12 GGT>TGT (G12C)	15%	20%	11%		59%
Mean $\pm$ SD			25%		
			18.0% $\pm$ 9.9%		
Codon 13	20% GGC>GAC (G13D)			37% GGC>AGC (G13S)	51% GGC>AGC (G13S)
Codon 61 Mean $\pm$ SD	29% CAA>CGA (Q61R)	54% CAA>CAC (Q61H)	29% CAA>CGA (Q61R)	42% CAA>CGA (Q61R)	89% CAA>CGA (Q61R)
	49% CAA>CTA (Q61L)			58% CAA>CAT (Q61H)	
	39.0% $\pm$ 14.1%			50.0% $\pm$ 11.3%	

NOTE. The mean PanIN concentrations of mutant *KRAS* increased with increasing grade of PanINs in each type of mutation. SD, standard deviation.

**Supplementary Table 4.** Results of *KRAS* and *GNAS* Mutation Analysis of the Second Set of PanINs

	Sex	Age, y	PanIN	Pathologic diagnosis	<i>KRAS</i>	<i>GNAS</i>
1	Female	68	PanIN-2	Ductal adenocarcinoma	G12D	None detected
2	Female	64	PanIN-1	Ductal adenocarcinoma	G12D	R201H
3	Male	70	PanIN-3	Ductal adenocarcinoma	G12D	None detected
4	Female	66	PanIN-2	Ductal adenocarcinoma	None detected	None detected
5	Male	76	PanIN-1	Pancreatic endocrine neoplasm	None detected	None detected
6	Male	57	PanIN-2	IPMN	G12D, G12V	None detected
7	Female	50	PanIN-2	Serous cystadenoma	G12D, G12V	R201H
8	Female	61	PanIN-2	Cholangiocarcinoma	G12V	None detected
9	Female	67	PanIN-1	Colloid adenocarcinoma	G12R	None detected
10	Male	74	PanIN-3	Ductal adenocarcinoma	G12R	None detected
11	Female	74	PanIN-3	IPMN	G12R	R201H
12	Female	74	PanIN-3	IPMN	G12R	None detected
13	Female	57	PanIN-1	Ductal adenocarcinoma	G12R	R201H
14	Female	75	PanIN-1	Cholangiocarcinoma	G12D, G12V	R201H
15	Female	75	PanIN-2	Cholangiocarcinoma	G12D	R201H
16	Female	75	PanIN-3	Cholangiocarcinoma	G12R, G12D, G12V	None detected
17	Female	76	PanIN-2	Ductal adenocarcinoma	G12V, G12D	None detected
18	Male	67	PanIN-1	Ampullary adenocarcinoma	G12V	None detected
19	Male	71	PanIN-2	Pancreatic endocrine neoplasm	G12D	None detected
20	Female	72	PanIN-2	Ductal adenocarcinoma	G12R	None detected
21	Female	57	PanIN-2	Ductal adenocarcinoma	G12V	None detected
22	Male	67	PanIN-1	Ductal adenocarcinoma	G12D	R201H, R201C
23	Female	49	PanIN-1	Ductal adenocarcinoma	G12V	None detected
24	Female	79	PanIN-2	Ductal adenocarcinoma	G12V	None detected
25	Female	57	PanIN-2	Ductal adenocarcinoma	G12V, G12R	None detected
26	Male	58	PanIN-3	IPMN	G12D	None detected
27	Female	58	PanIN-2	Ductal adenocarcinoma	G12R	None detected
28	Female	58	PanIN-3	Ductal adenocarcinoma	G12R	None detected
29	Male	56	PanIN-2	IPMN	G12R	None detected
30	Female	40	PanIN-1	Pancreatic endocrine neoplasm	G12D, G12V	None detected
31	Female	56	PanIN-1	Serous cystadenoma	G12D, G12V	None detected
32	Male	46	PanIN-2	Serous cystadenoma	G12D	None detected
33	Female	76	PanIN-2	Serous cystadenoma	G12D, G12V	None detected
34	Male	61	PanIN-2	GI stromal tumor (GIST) (duodenum)	G12V	None detected
35	Male	62	PanIN-2	IPMN	G12D	None detected
36	Female	79	PanIN-1	Ampullary adenocarcinoma	G12R	None detected
37	Female	79	PanIN-2	Ampullary adenocarcinoma	G12R	None detected

NOTE. Combining this set with the first set of PanIN results, *GNAS* mutations were still more common in patients with a primary diagnosis other than pancreatic cancer ( $P = .02$ ).

**Supplementary Table 5.** Primers and Annealing Temperatures Used for Polymerase Chain Reactions in This Study

Gene	Target	Experiment	Type	Oligo sequence (5'–3')	Product size	Annealing temperature
<i>KRAS</i>	Codon 12/13	Pyrosequencing	Forward	AGGCCTGCTGAAAATGACTG	119 bp	52°C
		Pyrosequencing	Reverse	TTGTTGGATCATATTCGTCCAC		
		Pyrosequencing	Sequencing	GTGGTAGTTGGAGCT		
	HRM	HRM	Forward	AGGCCTGCTGAAAATGACTG	119 bp	65°C
		HRM	Reverse	TTGTTGGATCATATTCGTCCAC		
		<i>KRAS</i> amplification	Forward	AGGCCTGCTGAAAATGACTG	119 bp	60°C
	Codon 61	<i>KRAS</i> amplification	Reverse	TTGTTGGATCATATTCGTCCAC		
		Pyrosequencing	Forward	CAGACTGTGTTTCTCCCTTCTCA	131 bp	62°C
		Pyrosequencing	Reverse	CTCATGACTGGTCCCTCGTTG		
	Codon 146	Pyrosequencing	Sequencing	ATATTCTCGACACAGCAG		
Pyrosequencing		Forward	AGTTAAGGACTCTGAAGATG	157 bp	56°C	
Pyrosequencing		Reverse	AGTGTACTTACCTGTCTTG			
Pyrosequencing	Sequencing	GAATTCCTTTTATTGAAAC				
<i>BRAF</i>	Codon 600	Pyrosequencing	Forward	ATGCTTGCTCTGATAGGAA	228 bp	59°C
		Pyrosequencing	Reverse	GCATCTCAGGGCCAAA		
		Pyrosequencing	Sequencing	TGATTTTGGTCTAGCTAC		
<i>GNAS</i>	Codon 201	Pyrosequencing	Forward	CTGTTTCGGTTGGCTTTGGTG	188 bp	63°C
		Pyrosequencing	Reverse	AGGGACTGGGGTGAATGTCAAG		
		Pyrosequencing	Sequencing	AGGACCTGCTTCGCTG		
<i>p16/CDKN2A</i>	Exon 1	HRM	Forward	GAAGAAAGAGGAGGGGCTG	340 bp	65°C
		HRM	Reverse	GCGCTACCTGATTCCAATTC		
	Exon 2	HRM	Forward	ACCCTGGCTCTGACCAT	316 bp	65°C
		HRM	Reverse	GCGGGCATGGTTACTGCCTCTG		

NOTE. Primers used for the ligation assay and BEAMing are provided in Wu et al.<sup>4</sup>  
 HRM, high-resolution melt curve assay.